

## APPLICATION OF SIMILARITY METHOD OF DISTANCE COURSES DESCRIBING THE ELEMENTS CONTENT IN PAVEMENT QUALITY CONCRETE

**Malgorzata Linek**

*Kielce University of Technology  
Faculty of Civil Engineering and Architecture  
Department of Transportation Engineering  
Państwa Polskiego Av. 7, 25-314 Kielce, Poland  
tel.: +48 41 3424844  
e-mail: linekm@tu.kielce.pl*

**Piotr Nita**

*Air Force Institute of Technology  
Ksiecica Boleslawa Street 6, 01-494 Warsaw, Poland  
tel.: +48 22 261851424, fax: +48 22 8364471  
e-mail: piotr.nita@itwl.pl*

### **Abstract**

*The publication presents the application of similarity analysis of distance courses. This method has been applied to define similarity of cement concrete intended for airfield pavements. The scope of works included standard concretes intended for airfield pavements and concretes after frost resistance test. The test has been conducted in diversified media used in the course of winter maintenance. The nature of resistance of pavement quality concrete was discussed with respect to frost resistance thereof. Research procedure was presented and the obtained laboratory tests results were discussed. Concrete samples were subject to observations using scanning electron microscope in order to define changes occurring in the internal microstructure. Chemical microanalysis of concrete composition before, in the course of and after the frost resistance test and the occurring changes were specified. The obtained laboratory tests results were intended for the purposes of the similarity analysis. Results obtained in case of standard pavement quality concrete were considered as comparative values. Characteristics of the remaining concretes were referred to these values and then similarity of distance courses were analysed. It was proved that  $BW_{M1}$  concrete was the most similar concrete to the comparative concrete.*

**Keywords:** *cement concrete, airfield pavement, analysis of similarity*

### **1. Purpose and scope**

The publication presents the application of similarity analysis of distance courses. This method was used to define similarities of cement concrete intended for airfield pavements. Due to operating conditions of airfield pavements [2], the significant element with respect to its durability is frost resistance of concrete composite. During the first stage of tests, the composition was developed and cement concrete intended for airfield pavements was prepared. The designed concrete complied with the requirements of [3], and the mix curve was consistent with good grain size distribution – Fig. 1. Composition of BW concrete included [1]: cement [4] in the quantity of  $370 \text{ kg/m}^3$ , sand in the quantity of  $390 \text{ kg/m}^3$ , granite grit fraction 2/8 mm in the quantity of  $510 \text{ kg/m}^3$ , granite grit fraction 8/16 mm in the quantity of  $430 \text{ kg/m}^3$ , granite grit fraction 16/32 mm in the quantity of  $442 \text{ kg/m}^3$ , water [5] in the quantity of  $148 \text{ kg/m}^3$ , air entraining agent –  $1.74 \text{ kg/m}^3$  and plasticizing admixture –  $0.63 \text{ kg/m}^3$ .

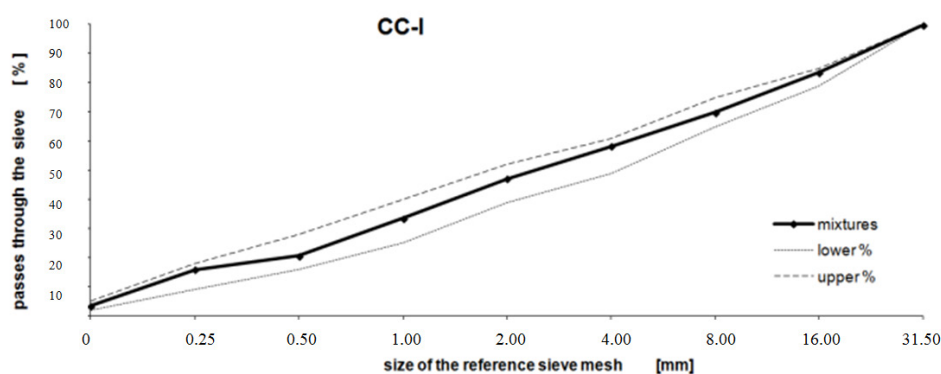


Fig. 1. Designed aggregate mixtures curve, together with limit curves (lower and upper)

In the course of laboratory tests, the parameters of concrete mixes and hardened mixes were determined. Air content ( $p$ ), according to [6], were defined for the designed concrete mixes. Compression strength ( $f_{ck}$ ) [7] in case of hardened concrete was determined. Then, concrete samples were intended for defining frost resistance. The method included freezing and defrosting cycles alternately. Conducted analysis referred to frozen and defrosted samples for 200 cycles. Single freezing cycle within testing included temperature ranging to  $-18^{\circ}\text{C}$  for the period of four hours, and then defrosting in water of the  $18^{\circ}\text{C}$  temperature. Frost resistance cycles were conducted in three media. The first series of samples was stored in water (symbol  $\text{BW}_W$ ) in compliance with the requirements of [3]. The second series was exposed to the destructive influence of carbamide (symbol  $\text{BW}_{Mt}$ ). While the third series was stored in potassium formate (symbol  $\text{BW}_{Mr}$ ). The decrease of weight ( $\Delta m$ ) and resistance ( $\Delta f_{ck}$ ) was determined after 200 frost resistance cycles for concretes stored in all types of media – Tab. 1. Internal structure of concrete composite was also assessed. Scanning electron microscope was used for this purpose. Fresh fractures were performed taking concrete samples; the preparation surface subject to SEM observations was not less than  $1.0\text{ cm}^2$ . The extent of magnification was from  $200\times$  to  $100000\times$ . Chemical microanalyses of selected sections in concrete composite were performed, as well. The results obtained during this stage served as the basis for the analysis of similarity of distance courses of analysed concretes.

## 2. Test results and their analysis

The obtained concrete test results after 28 days of curing and subject to 200 frost resistance cycles were presented in the Tab. 1.

Tab. 1. Parameters of mixtures and concretes

concrete	parameters			
	$p$	$f_{ck}$	$\Delta f_{ck}$	$\Delta m$
	[%]	[MPa]	[%]	[%]
BW	4.5	57.0	-	-
$\acute{s}w\text{BW}_W$	4.5	63.6	11.3	4.0
$\text{BW}_W$	4.5	59.5	5.2	2.9
$\acute{s}w\text{BW}_{Mt}$	4.5	77.0	26.7	4.3
$\text{BW}_{Mt}$	4.5	72.2	21.9	4.1
$\acute{s}w\text{BW}_{Mr}$	4.5	61.8	8.6	3.3
$\text{BW}_{Mr}$	4.5	51.4	9.7	3.5

Based on observations of fractures of BW concretes stored in liquids (witnessing –  $\acute{s}w\text{BW}$ ) and exposed to the influence of freezing cycles it was proved that the internal structure has changed. Significant diversification occurs in case of crystallization within the area of cement matrix, contact area between cement matrix and aggregate grains and porosity characteristics of both concretes.

Microstructure of  $^{sw}BW_{Mr}$  concretes with respect to BW concretes proved the reduction of air voids in cement matrix. Within contact area between quartz grains and cement matrix of  $^{sw}BW_{Mr}$  concrete, the cracks occurred and the width of scratches extended in matrix. Matrix of  $^{sw}BW_{Mr}$  concrete is distinguished by the reduced diameters of voids.

Microstructure of  $BW_{Mr}$  concretes with respect to BW concretes is distinguished by the reduced number of voids in fine-grained cement matrix. Inside the voids, ettringite crystallization takes place. There are scratches within the area of air voids walls and contact areas between voids and cement matrix.

Microstructure of  $^{sw}BW_{Mt}$  concretes in comparison to BW concretes is distinguished by the increased width of scratches of cement matrix. Within the contact area between quartz grains and matrix, the occurrence of silicates and portlandite in layers was observed, which are missing in the microstructure of BW concrete. In case  $^{sw}BW_{Mt}$  concretes, there is no network ettringite crystallization; however, there are parallel ettringite crystals and tile crystallization. Almost double increase of cracks width within contact areas between coarse aggregate grains and cement matrix was observed.

Microstructure of  $BW_{Mt}$  concretes in comparison to BW concretes is distinguished by the increased diameters of voids and increased width of scratches. Within the contact area between quartz grains and matrix, scratches increased and locally more developed crystallization of ettringite occurs. Inside voids, the changed crystallization takes place – no network of ettringite crystals, while there are carbonated ettringite crystals.

Data obtained as a result of chemical microanalysis (average values of 6 analyses) of concretes was subject to similarity analysis [1]. As an input sequence in similarity analysis, BW characteristics values obtained were assumed. The data, which reflect the percentage of selected elements in one of  $^{sw}BW$  reference concrete sections, play the role of target sequence, which input sequence is compared. Average value of all D matrix elements was defined as similarity measurement of both sequences. The matrix D represents the distance between input and output values. The element  $d_{ij}$  of matrix D, located within the intersection i-of this line and j-of this column D. Refers to the distance i-of this value of input sequence and j-of this value of target sequence. Average value of all D matrix elements was defined as similarity measurement of both sequences. Due to the failure to take into consideration the arrangement of sequence values, similarity measurement was performed in the next stage. According to this measurement, various paths leading through the matrix from element (1.1) to element ( $n_x, n_y$ ) were compared. The path was determined, which leads from the least average distance along the path.

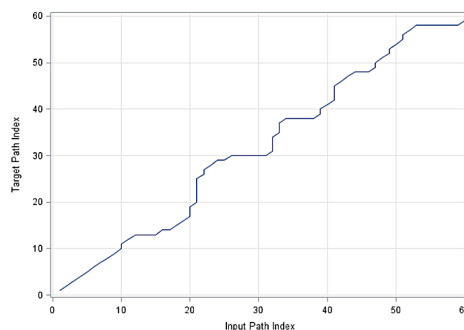


*Fig. 2. Path leading to the smallest distance between the input and target sequences – carbon / contact area between fine aggregate grains and cement matrix*

Distances were determined (Fig. 3) between the values of input and target sequences along the optimal path. Determined distance histogram between input and target sequences along optimal path with the indicated Gauss's curve and nuclear density curve (Fig. 4).

According to the conducted analysis, similarity index was obtained between the input and target sequences along the optimal path. In case of data before standardization, it is 1.278, while in case of data after the standardization it is 0.438.

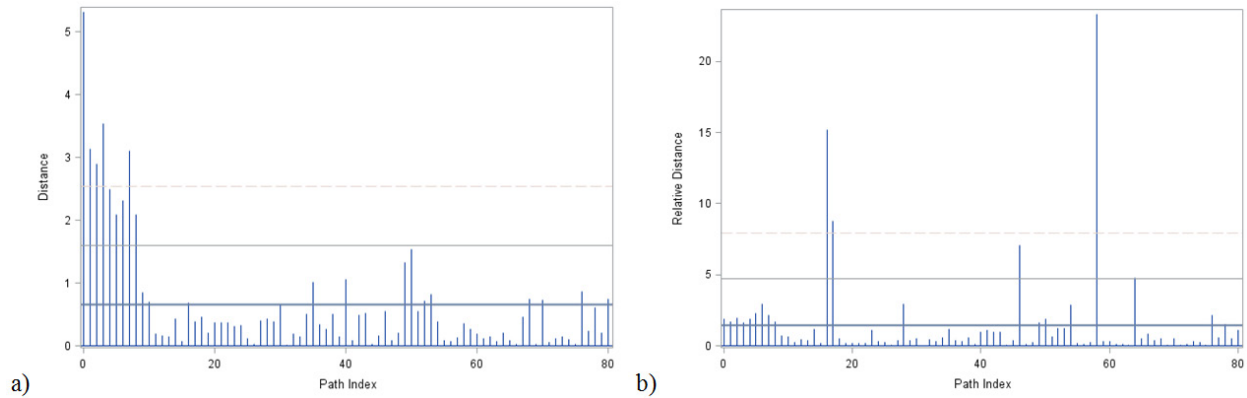


Fig. 3. Distance between the input and target sequences along optimal path: a) data prior to standardization, b) data after standardization

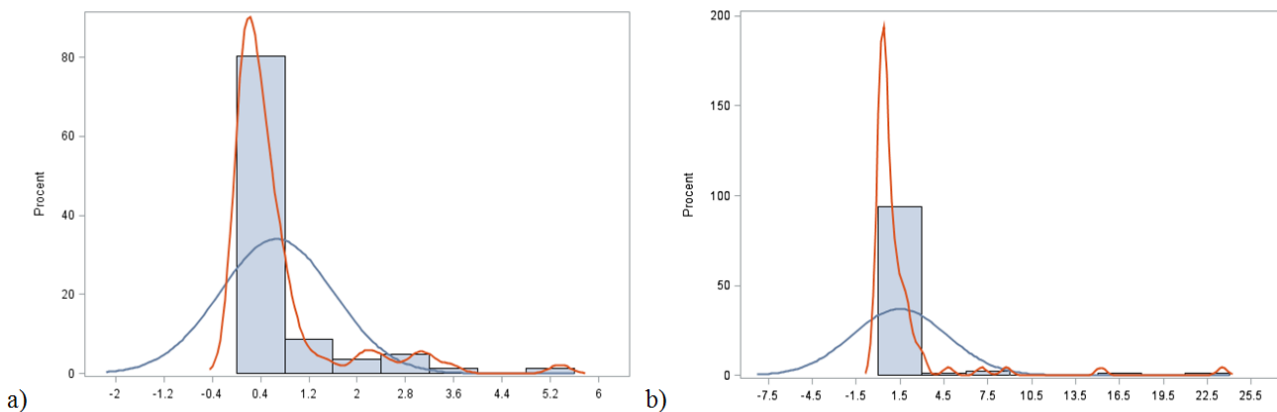


Fig. 4. Histogram of distance between standardized input sequences and standardized target sequences along optimal path with indicated Gauss's curve (blue) and nuclear density curve (red): a) data prior to standardization, b) data after standardization

Analyses included the diversification in terms of contents of carbon, oxygen, aluminium, silicon, sulphur, potassium, calcium, iron, sodium and magnesium. The data for four various section were analysed. As the first section, cement matrix was taken into consideration. The three remaining sections included contact areas between cement matrix and grains of granite aggregate, grains of quartz aggregate and air voids. Determined similarity indexes were included in Tab. 2. These indexes allow assessing similarity of each concrete in terms of contents of individual elements in the analysed sections.

Obtained similarity indexes were used as the basis to prepare diagrams of „proximity” of distance courses. The polygon method was applied, in which the number of sides corresponds to the number of attributes used in case of structure description.

The first stage was to arrange values of each attribute, and then the length of radii was calculated. These radii indicate vertices of individual polygons. It was assumed that attributes are similarity indexes of distance courses of concrete and BW concrete for the subsequent elements in the defined section. The object of the minimum attribute value corresponds with the shortest radius towards this attribute. The object of the greatest attribute value had the longest radius. The remaining values of attributes were converted linearly within the length of radii coming from the centre of polygon towards relevant attributes. It was assumed that values of the first attribute correspond to the radius of Ox axis direction. Next attributes are located on the subsequent radii, counted from the first one counter-clockwise, and counted from the first one counter-clockwise. Shape and size of a single polygon reflects how a given object is presented in comparison with other objects described by means of the same attributes. Higher polygon proves smaller similarity of concrete to the reference concrete BW.

Tab. 2. The list of similarity indexes  $w_p$  for selected areas

concrete	elements									
	C	O	Al	Si	S	K	Ca	Fe	Na	Mg
	First section: cement matrix									
$\acute{s}wBW_{Mr}$	0.450	0.447	0.467	0.445	0.000	0.450	0.326	0.311	0.767	0.717
$BW_{Mr}$	0.359	0.328	0.442	0.434	0.000	0.439	0.371	0.291	0.821	0.791
$\acute{s}wBW_{Mt}$	0.416	0.440	0.293	0.461	0.000	0.557	0.496	0.213	0.723	0.788
$BW_{Mt}$	0.408	0.468	0.416	0.450	0.812	0.475	0.426	0.278	0.851	0.831
	Section: contact area between air pores and cement matrix									
$\acute{s}wBW_{Mr}$	0.288	0.315	0.406	0.325	0.417	0.515	0.290	0.497	0.696	0.775
$BW_{Mr}$	0.385	0.429	0.449	0.474	0.851	0.471	0.444	0.401	0.539	0.494
$\acute{s}wBW_{Mt}$	0.442	0.827	0.710	0.410	0.448	0.617	0.419	0.598	0.594	0.539
$BW_{Mt}$	0.553	0.408	0.416	0.400	0.596	0.450	0.636	0.297	0.696	0.775
	Section: contact area between fine aggregate and cement matrix									
$\acute{s}wBW_{Mr}$	0.704	0.652	0.179	0.251	0.816	0.459	0.282	0.316	0.000	0.000
$BW_{Mr}$	0.627	0.367	0.478	0.592	0.623	0.424	0.332	0.221	0.683	0.000
$\acute{s}wBW_{Mt}$	0.391	0.408	0.304	0.374	0.749	0.348	0.464	0.239	0.000	0.000
$BW_{Mt}$	0.357	0.403	0.292	0.419	0.643	0.543	0.462	0.194	0.000	0.000
	Section: contact area between coarse aggregate and cement matrix									
$\acute{s}wBW_{Mr}$	0.390	0.510	0.400	0.472	0.696	0.477	0.461	0.487	0.000	0.000
$BW_{Mr}$	0.491	0.380	0.466	0.673	0.000	0.443	0.411	0.386	0.000	0.677
$\acute{s}wBW_{Mt}$	0.495	0.450	0.427	0.702	0.763	0.542	0.504	0.495	0.000	0.789
$BW_{Mt}$	0.408	0.352	0.363	0.331	0.857	0.362	0.339	0.365	0.838	0.870

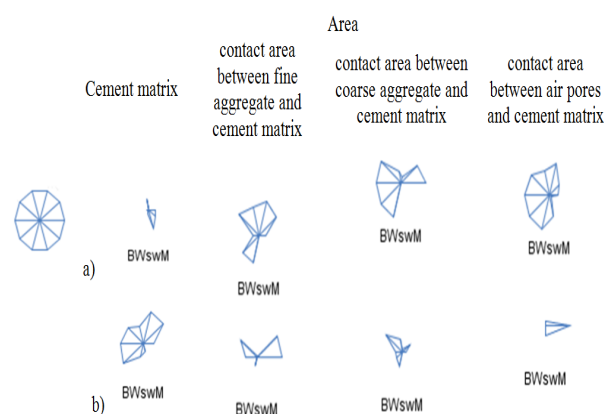


Fig. 5. The polygon method: a) data prior to standardization, b) data after standardization –  $\acute{s}wBW_{Mt}$

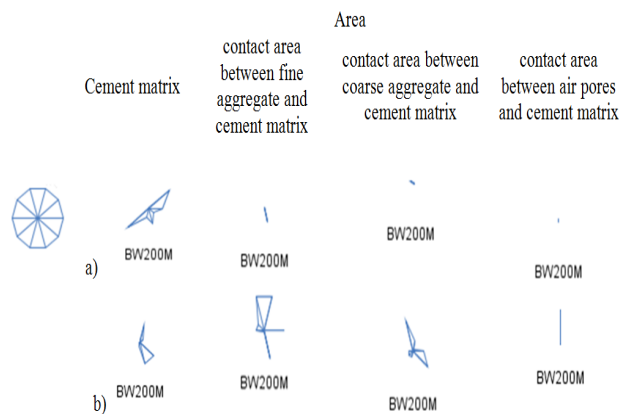


Fig. 6. The polygon method: a) data prior to standardization, b) data after standardization –  $BW_{Mt}$

Based on the obtained distance courses, it was proved that the standardization of results has significant influence on the obtained results.

Analysing the data before the standardization it was proved that the contact area between fine aggregate grains and cement matrix of  $\acute{s}wBW_{Mr}$  concrete is distinguished by the most similar nature of distance courses to the reference concrete. In case of concrete  $BW_{Mr}$ , contact areas between fine and coarse aggregate grains and cement matrix are distinguished by the most similar nature of distance courses to the reference concrete. In case of  $BW_{Mt}$  concrete, the contact areas between fine and coarse aggregate grains and between air voids and matrix are distinguished by the most similar nature of distance courses to the reference concrete. The highest diversification was proved in case of cement matrix.

In the event of data subject to standardization, the most significant differences were found within the matrix area ( $\acute{s}wBW_{Mt}$ ,  $\acute{s}wBW_{Mr}$  and  $BW_{Mr}$ ) and contact area between the matrix and fine aggregate grains ( $BW_{Mt}$ ) Changes of internal structure of concrete composite determined on the basis of the observation conducted by means of scanning electron microscope were proved.

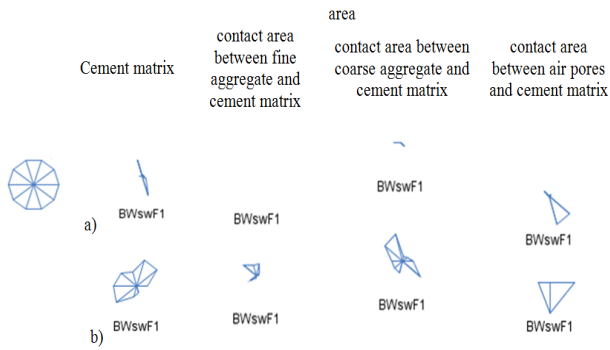


Fig. 7. The polygon method: a) data prior to standardization, b) data after standardization –  ${}^{\text{sw}}\text{BW}_{\text{Mr}}$

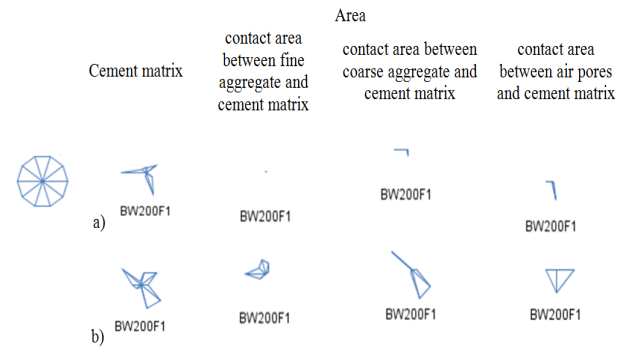


Fig. 8. The polygon method: a) data prior to standardization, b) data after standardization –  $\text{BW}_{\text{Mr}}$

### 3. Conclusions

Pursuant to the obtained test results, the following conclusions were drawn:

- compressive strength of hardened concrete has changed as a result of storage in carbamide, water and potassium formate (the increase of resistance by 4.8 MPa in case of concrete  ${}^{\text{sw}}\text{BW}_{\text{Mt}}$ , increase of resistance by 6.6 MPa in case of concrete  ${}^{\text{sw}}\text{BW}_{\text{W}}$  and increase of resistance by 20 MPa in case of concrete  ${}^{\text{sw}}\text{BW}_{\text{Mt}}$ ),
- compressive strength of hardened concrete has changed as a result of influence of freezing and defrosting cycles (the increase of resistance by 2.5 MPa in case of concrete  ${}^{\text{sw}}\text{BW}_{\text{W}}$ , decrease of resistance by 5.6 MPa in case of concrete  ${}^{\text{sw}}\text{BW}_{\text{Mr}}$  and increase of resistance by 15.2 MPa in case of concrete  ${}^{\text{sw}}\text{BW}_{\text{Mt}}$ ),
- characteristics of internal micro structure of concrete stored in carbamide and potassium formate with respect to the comparative concrete has changed,
- characteristics of internal micro structure of concrete after 200 frost resistance cycles in carbamide and potassium formate with respect to the comparative concrete has changed,
- concrete  $\text{BW}_{\text{Mt}}$  within the contact area between fine aggregate grains and cement matrix is the most similar to the reference  $\text{BW}$  concrete, in terms of distance courses.

### References

- [1] Linek, M. *Surface concrete with improved parameters of physical and mechanical on the loads caused by forced temperature*, PhD Thesis, Kielce 2013.
- [2] Nita, P. *Concrete surface airport. Theory and structural dimensioning*, Publishing Air Force Institute of Technology, Warsaw 2005.
- [3] NO 17-A204:2015 *Airfield concrete pavements – Requirements and test methods for cement concrete pavements* – Polish standard 2015.
- [4] PN-EN 197-1:2012 *Cement, part 1: Composition, specifications and conformity criteria for common cements* – Polish standard.
- [5] PN-EN 1008:2004 *Mixing water for concrete – Specification for sampling, testing and assessing the suitability of water, including water recovered from processes in the concrete industry, as mixing water for concrete* – Polish standard 2004.
- [6] PN-EN 12350-7:2011 *Testing fresh concrete. Part 7: Air content – Pressure methods* – Polish standard 2011.
- [7] PN-EN 12390-3:2011 *Testing hardened concrete – Part 3: Compressive strength of test specimens* – Polish standard 2011.